AIAA JOURNAL
Vol. 32, No. 8, August 1994

New Higher Order Plate Theory in Modeling Delamination Buckling of Composite Laminates

Aditi Chattopadhyay* and Haozhong Gu†
Arizona State University, Tempe, Arizona 85287

A new higher order plate theory for modeling delamination buckling and postbuckling of composite laminates is developed. Delaminations between layers of composite plates are modeled by jump discontinuity conditions, in both lower and higher order terms of displacements, at the delaminated interfaces. Some higher order terms are identified at the beginning of the formulation by using the conditions that shear stresses vanish at all free surfaces including the delaminated interfaces. Therefore, all boundary conditions for displacements and stresses are satisfied in the present theory. Geometric nonlinearity is included in computing layer buckling. The general governing equations, along with all boundary and continuity conditions of plates, are derived for predicting the delamination buckling and postbuckling behavior. The associated delamination growth problem is also examined by the use of Griffith-type fracture criterion. A numerical example is presented to validate the theory. The results are also compared with experimentally obtained data.

Nomenclature

E_L, E_T = elastic moduli of lamina in longitudinal and transverse directions, respectively
$\bar{G}$ = normalized energy release rate
G_{LT}, G_{TT} = shear moduli in the plane, perpendicular and parallel to longitudinal direction of lamina, respectively
$G(\beta)$ = strain energy release rate
$H(h_1)$ = step function
h = plate thickness
h_1 = distance from plate mid-plane to delamination interface
L = plate length
N = number of the order used to evaluate the transverse shear effect
$N_{ij}^{(k)}$ = stress resultants, $i = 1, 2, \ldots, 6; j = 1, 2, \ldots, N; k = 0, 1, 2$
n_x, n_y = components of normal vector of plate boundary
$\bar{P}$ = normalized axial compressive load
p = inplane compressive load distribution
$\bar{p}$ = nondimensional critical load, (normalized with respect to solution from classical lamination theory)
$\bar{Q}_{ij}$ = stiffness components of lamina, $i, j = 1, 2, \ldots, 6$
U = strain energy
U_{ij}, V_{ij}, W_i = jth order displacement functions, $i = 0, 1, 2; j = 1, 2, \ldots, N$
u_i = displacement components, $i = 1, 2, 3$
$\bar{W}_1$ = normalized midpoint deflection of bottom layer
$\bar{W}_2$ = normalized midpoint deflection of upper layer
α = thickness parameter of delamination layer, $2h_1/h$
βL = delamination length
Γ_σ = plate boundary in which the compressive load is applied
Γ_Ω = boundary of plate
Γ_{Ω_d} = interfaces between delamination region and nondelamination region
ε_i = strain components, $i = 1, 2, \ldots, 6$
ν_{LT}, ν_{TL} = Poisson's ratio in longitudinal and transverse directions, respectively
ξ_i, ζ_j, η_j = functions of coordinate variable z, $i = 1, 2, \ldots, N-1$; $j = 1, 2, \ldots, 2N-2$
Π = total potential energy
σ_i = stress components, $i = 1, 2, \ldots, 6$
φ_{im}, ψ_{im} = identified functions of displacements, $i = 0, 1, 2$; $m = N-1, N$
Ω = region of whole plate
Ω_d = delamination region of plate

Received Aug. 14, 1993; revision received Feb. 1, 1994; accepted for publication Feb. 5, 1994.

*Assistant Professor, Department of Mechanical and Aerospace Engineering. Senior Member AIAA.
†Graduate Research Assistant, Department of Mechanical and Aerospace Engineering. Member AIAA.

Introduction

WITH the increasing use of composite materials, problems of delamination have received wide attention in recent years. Delaminations develop as a result of imperfections in production technology or discontinuous interlaminar stresses during the operational life. The presence of delaminations may allow laminate failure initiated by delamination buckling and thus greatly reduce the load-carrying capacity of the laminates.

A large number of recent studies have analytically investigated the delamination buckling phenomenon for both a one-dimensional, through-the-width, and a two-dimensional, embedded delamination. In an early study Chai et al.[1] and Chai and Babcock[2] analyzed the behavior of an interlayer crack close to the surface in a thick compressed substrate. Whitcomb[3] used a finite element method to compute the crack closure integral. In the so-called thin film analysis, postbuckling of cracked laminates was determined and eventual crack growth predicted based on a Griffith criterion. In this spirit Sallam and Simitses[4] extended the work to truly laminated configurations and discussed the effect of coupling between bending and stretching on delamination growth.

For the work just mentioned, the effects of transverse shear on delamination buckling and growth are seldom considered. However, the effects of transverse shearing stresses are important for composite laminates because, in composite fiber-reinforced materials, the interlaminar shear moduli are usually much smaller than the inplane Young's moduli. For a laminated plate subjected to bending loads the solutions based on classical lamination theory showed significant departures from the exact elasticity solutions for the cases with low ratios of inplane dimensions to thickness.[5] As a result, it is necessary to use a shear deformation theory to deal with the problem for a moderately thick plate. Recently, Kardomateas and Schmueser[6] performed some studies about the effects of transverse shearing forces on the buckling of delaminated composites under compressive loads. Their studies were based on the classical engineering solutions of beam columns with linear transverse shear correction terms added to account for shear effects. Chen[7] used a variational energy principle approach to formulate a similar problem. The latter work is more general and more systematic in formulation.

A more general theory for the modeling of delamination in composite laminates, based on a layer-wise displacement field, was presented by Barbero and Reddy.[8] They suggested that the same displacement distributions in an individual layer are capable of representing displacement discontinuity conditions at interfaces between layers. The study demonstrated that the layer-wise laminate theory provides an adequate framework for the delamination analysis of laminated composites. It must be noted, however, that the computational cost of the analysis makes it unattractive for the prediction of delamination buckling behavior in engineering practice when the number of layers is large.

In studying composite delamination, it is important to have a more effective general theory for accurately evaluating the transverse shear effects. It has long been recognized that higher order plate theory provides an effective solution tool for accurately predicting the deformation behavior of composite laminates subjected to bending loads. However, no research has been reported in which an attempt has been made to extend the higher order theory to model the problem of delamination. The difficulty in such a formulation is obvious. It is difficult to provide the consistent displacement field which satisfies the transverse shear stress boundary conditions at all free surfaces including the debonding intersurfaces in delamination regions.

To address this issue, a new higher order plate theory is proposed for modeling the delamination problem. The displacement field of regular higher order theory[5] is modified and used. An appropriate kinematic description which allows for separation and slipping is required to model the delamination in laminated composite plates.[8] In this paper, both the lower and the higher order terms are employed to describe the separation and slipping for the delamination layer and the substrate. To satisfy all of the transverse shear stress boundary conditions, some higher order shear correction terms are eliminated to meet the specific need for a delamination-type problem. All of these considerations make the displacement description presented here appropriate for predicting all possible instability modes associated with delamination buckling. The proposed theory can be applied to both one-dimensional, through-the-width, and two-dimensional, embedded delaminations which are entirely separated from each other after buckling. Numerical results are presented and are compared to experimentally obtained data and existing solutions .

New Higher Order Laminate Plate Theory for Delamination

Displacement, Strain, and Stress

Consider the general inplane loading of a laminate plate containing an arbitrary shape of delamination (Fig. 1). To describe all possible kinematical behavior of the delamination buckling of a laminate plate, the following displacement field is used through the thickness of the plate:

$$u_1(x,y,z) = \sum_{j=0}^{N} z^j \{U_{0j}(x,y) + [1-H(h_1)]\,U_{1j}(x,y) + H(h_1)\,U_{2j}(x,y)\}$$

$$u_2(x,y,z) = \sum_{j=0}^{N} z^j \{V_{0j}(x,y) + [1-H(h_1)]\,V_{1j}(x,y) + H(h_1)\,V_{2j}(x,y)\} \tag{1}$$

$$u_3(x,y,z) = W_0(x,y) + [1-H(h_1)]\,W_1(x,y) + H(h_1)W_2(x,y)$$

where (U_{00}, V_{00}, W_0) are the displacements of a point (x, y) on the midplane, $(U_{0j}, V_{0j}; j = 1, 2, \ldots, N)$ are the jth order transverse shear correction terms, and $H(h_1)$ is the Heaviside step function described as

$$H(h_1) = H(z-h_1) = \begin{cases} 1 & z \geq h_1 \\ 0 & z < h_1 \end{cases} \tag{2}$$

The jumps in displacements between the sublaminate layer and the buckling layer are given by (U_{1j}, V_{1j}) and (U_{2j}, V_{2j}), $j = 0, 1, \ldots, N$, respectively. Note that the terms related to the delamination (U_{ij}, V_{ij}), $i = 1, 2$, only exist in the delamination region Ω_d. The use of the step function $H(h_1)$ allows the kinematic description for separation and slipping due to the independence of the displacements, shown in Eq. (1), on adjacent layers at the delamination interface.

Considering the fact that the rotations and the displacements are not expected to be so large as to require a full nonlinear analysis, the von Kármán-type of nonlinearity in the kinematic equation is used here.

$$\begin{aligned} \varepsilon_1 &= \varepsilon_{11} = \frac{\partial u_1}{\partial x} + \frac{1}{2}\left(\frac{\partial u_3}{\partial x}\right)^2 \\ \varepsilon_2 &= \varepsilon_{22} = \frac{\partial u_2}{\partial y} + \frac{1}{2}\left(\frac{\partial u_3}{\partial y}\right)^2 \\ \varepsilon_4 &= 2\varepsilon_{23} = \frac{\partial u_2}{\partial z} + \frac{\partial u_3}{\partial y} \\ \varepsilon_5 &= 2\varepsilon_{13} = \frac{\partial u_1}{\partial z} + \frac{\partial u_3}{\partial x} \\ \varepsilon_6 &= 2\varepsilon_{12} = \frac{\partial u_1}{\partial y} + \frac{\partial u_2}{\partial x} + \frac{\partial u_3}{\partial x}\frac{\partial u_3}{\partial y} \end{aligned} \tag{3}$$

The equations relating the stresses to the strains for the kth layer in a laminate coordinate (x, y, z) are expressed as follows:

$$\begin{bmatrix} \sigma_1 \\ \sigma_2 \\ \sigma_4 \\ \sigma_5 \\ \sigma_6 \end{bmatrix}_k = \begin{bmatrix} \bar{Q}_{11} & \bar{Q}_{12} & 0 & 0 & \bar{Q}_{16} \\ \bar{Q}_{12} & \bar{Q}_{22} & 0 & 0 & \bar{Q}_{26} \\ 0 & 0 & \bar{Q}_{44} & \bar{Q}_{45} & 0 \\ 0 & 0 & \bar{Q}_{45} & \bar{Q}_{55} & 0 \\ \bar{Q}_{16} & \bar{Q}_{26} & 0 & 0 & \bar{Q}_{66} \end{bmatrix}_k \begin{bmatrix} \varepsilon_1 \\ \varepsilon_2 \\ \varepsilon_4 \\ \varepsilon_5 \\ \varepsilon_6 \end{bmatrix}_k \tag{4}$$

where the quantities $\bar{Q}_{ij}$ are calculated in terms of the orthotropic stiffness, Q_{ij}, through the usual transformation techniques. The orthotropic stiffnesses expressed in terms of the engineering constants, E_i, ν_i, and G_{ij} $(i, j = 1, 2)$ can be found in Ref. 9.

Refined Displacement Field

It must be noted that the expression for displacement, as stated in Eq. (1), does not satisfy the transverse shear stress-free boundary conditions. These stress-free boundary conditions in delamination problems require that the transverse shear stresses σ_4 and σ_5 vanish on the plate top and bottom surfaces and on the debonding surfaces in the delamination region. That is,

$$\begin{aligned} &\sigma_4(x,y,\pm h/2) = 0, \quad \sigma_5(x,y,\pm h/2) = 0 \quad (x,y) \in \Omega \\ &\sigma_4^{\pm}(x,y,h_1) = 0, \quad \sigma_5^{\pm}(x,y,h_1) = 0 \quad (x,y) \in \Omega_d \end{aligned} \tag{5}$$

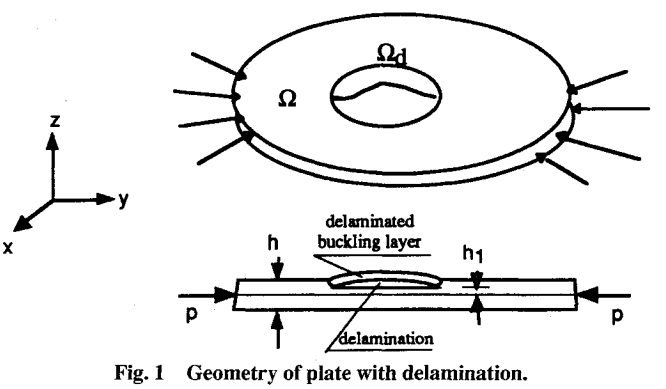

Fig. 1 Geometry of plate with delamination.

in which the superscripts "+" and "–" denote the quantities related to the buckling layer and sublaminate layer, respectively. For orthotropic plates, the conditions are equivalent to the requirement that the corresponding strains be zero on these surfaces. Therefore,

$$\varepsilon_4(x, y, \pm h/2) = 0, \quad \varepsilon_5(x, y, \pm h/2) = 0 \quad (x, y) \in \Omega$$
$$\varepsilon_4^{\pm}(x, y, h_1) = 0, \quad \varepsilon_5^{\pm}(x, y, h_1) = 0 \quad (x, y) \in \Omega_d \tag{6}$$

Applying these stress-free boundary conditions to Eq. (2), and using the displacement expression (1), some higher order terms can be identified in terms of lower order terms as follows.

$$U_{im}(x, y) = \varphi_{im}(x, y; U_{kj}, W_k)$$
$$V_{im}(x, y) = \psi_{im}(x, y; U_{kj}, W_k)$$
$$i = 0, 1, 2; \quad j = 1, 2, \ldots, N-2; \quad m = N-1, N$$
$$k = 0, \text{if } i = 0; \quad k = 0, i, \text{if } i \neq 0 \tag{7}$$

Using the preceding expression, the refined displacement field, which satisfies all of the boundary conditions, can be defined as follows.

$$\begin{aligned} u_1(x, y, z) &= \sum_{j=0}^{N-2} \xi_j(z)\, U_{0j}(x, y) + \xi_{N-1}(z)\, W_{0,x}(x, y) \\ &+ [1-H(h_1)] \left\{ \sum_{j=0}^{N-2} [\zeta_j(z)\, U_{1j}(x, y) + \zeta_{j+N}(z)\, U_{0j}(x, y)] \right. \\ &\left. + \zeta_{N-1}(z)\, W_{1,x}(x, y) + \zeta_{2N-1}(z)\, W_{0,x}(x, y) \right\} \\ &+ H(h_1) \left\{ \sum_{j=0}^{N-2} [\eta_j(z)\, U_{2j}(x, y) + \eta_{j+N}(z)\, U_{0j}(x, y)] \right. \\ &\left. + \eta_{N-1}(z)\, W_{2,x}(x, y) + \eta_{2N-1}(z)\, W_{0,x}(x, y) \right\} \end{aligned}$$

$$\begin{aligned} u_2(x, y, z) &= \sum_{j=0}^{N} \xi_j V_{0j}(x, y) + \xi_{N-1}(z)\, W_{0,y}(x, y) \\ &+ [1-H(h_1)] \left\{ \sum_{j=0}^{N-2} [\zeta_j(z)\, V_{1j}(x, y) + \zeta_{j+N}(z)\, V_{0j}(x, y)] \right. \\ &\left. + \zeta_{N-1}(z)\, W_{1,y}(x, y) + \zeta_{2N-1}(z)\, W_{0,y}(x, y) \right\} \\ &+ H(h_1) \left\{ \sum_{j=0}^{N-2} [\eta_j(z)\, V_{2j}(x, y) + \eta_{j+N}(z)\, V_{0j}(x, y)] \right. \\ &\left. + \eta_{N-1}(z)\, W_{2,y}(x, y) + \eta_{2N-1}(z)\, W_{0,y}(x, y) \right\} \end{aligned} \tag{8}$$

$$u_3(x, y, z) = W_0(x, y) + [1 - H(h_1)]\, W_1(x, y) + H(h_1) W_2(x, y)$$

In the present paper, $N = 4$ is used to formulate the displacement field. The specific form of the higher order terms (U_{im}, V_{im}) are derived in Appendix A.

Virtual Work and Governing Equations

Consider a plate that is subject to an inplane compressive load distribution, p, at the midplane in the direction normal to the boundary of the plate (Fig. 1). The minimum total potential energy principle is used to derive the governing equations and associated boundary conditions. The minimum total potential energy principle states that the variation of the total potential energy is equal to zero, that is,

$$\delta\Pi = \int_{\Omega} \int_{-h/2}^{h/2} \sigma_i \delta\varepsilon_i \, dz \, d\Omega - \int_{\Gamma_\sigma} p\,(n_x \delta U_{00} + n_y \delta V_{00}) \, d\Gamma = 0 \tag{9}$$

Equation (8) can be rewritten based on two integral regions, the nondelamination region $\Omega - \Omega_d$ and the delamination region Ω_d as follows.

$$\begin{aligned} &\int_{\Omega-\Omega_d} \int_{-h/2}^{h/2} \sigma_i^{(0)} \delta\varepsilon_i^{(0)} \, dz \, d\Omega + \int_{\Omega_d} \left[\int_{-h/2}^{h_1} \sigma_i^{(1)} \varepsilon_i^{(1)} \, dz \right. \\ &\left. + \int_{h_1}^{h/2} \sigma_i^{2} \varepsilon_i^{(2)} \, dz \right] d\Omega - \int_{\Gamma_\sigma} p\,(n_x \delta U_{00} + n_y \delta V_{00}) \, d\Gamma = 0 \end{aligned} \tag{10}$$

where the superscript 0 denotes the quantities related to only the nondelamination variables (U_{0j}, V_{0j}, W_0) in the displacement expression [Eq. (1)], and superscripts 1 and 2 denote the quantities related to the variables (U_{0j}, V_{0j}, W_0, U_{1j}, V_{1j}, W_1) and (U_{0j}, V_{0j}, W_0, U_{2j}, V_{2j}, W_2), respectively.

From the virtual work statement [Eq. (10)], the governing equations, the associated boundary conditions, and the continuity conditions are derived (see Appendix B) by using the refined displacement expressions, which are obtained by combining Eq. (A1) (Appendix A) and Eq. (1).

Delamination Growth

The deformation field obtained from the proposed theory is used to compute the strain energy release rate along the boundary of the delamination. It is assumed in the present work that the delamination growth will take place in its own plane and is governed by Griffith fracture criterion.

The virtual work extension method postulates that the strain energy release rate, $G(s)$, can be computed from the strain energy U and the crack area A (Fig. 2) as follows

$$G(s) = \frac{dU}{dA} \tag{11}$$

where the relative strain energy is given by

$$U = \int_{\Omega_d} \left[\int_{-h/2}^{h_1} (\sigma_i^{(1)} \varepsilon_i^{(1)} - \sigma_i^{(0)} \varepsilon_i^{(0)}) \, dz + \int_{h_1}^{h/2} (\sigma_i^{(2)} \varepsilon_i^{(2)} - \sigma_i^{(0)} \varepsilon_i^{(0)}) \, dz \right] d\Omega \tag{12}$$

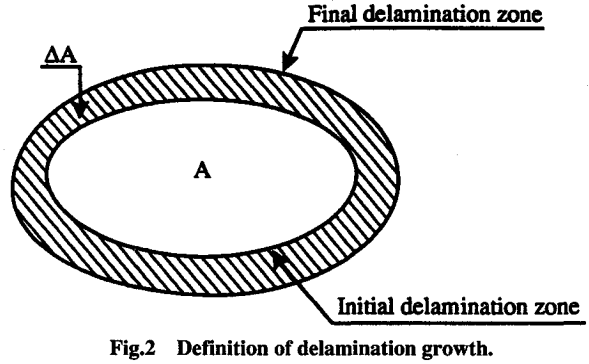

Fig.2 Definition of delamination growth.

For the plate of unit width with only a one-dimensional, through-the-width delamination, Eq. (11) can be simplified to

$$G(s) = \frac{1}{L}\frac{dU}{d\beta} \tag{13}$$

in which βL is the representative crack length.

Numerical Results and Discussion

An example of a plate with clamped ends and a midplane delamination[10] under axial compression is presented to validate the proposed theory. The plate has a nominal length L of 3 in. and a thickness h of 0.22 in. The material used in this example is a random short-fiber SMC-R50 composite whose properties are as follows.

$E_L = 1.58 \times 10^6$ psi $E_T = 1.1 \times 10^6$ psi $G_{LT} = 0.36 \times 10^6$ psi

$\nu_{LT} = 0.22$ $\nu_{TT} = 0.31$

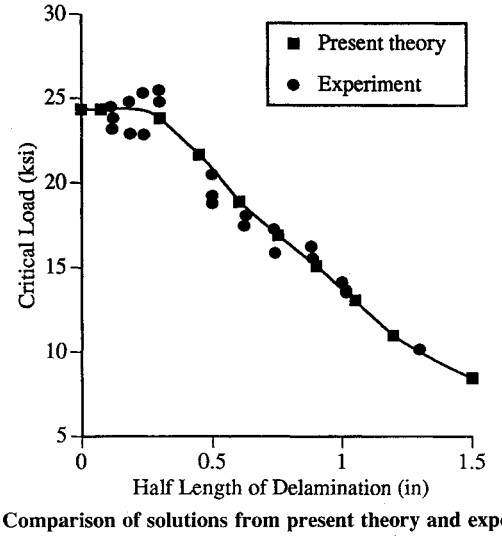

Fig. 3 Comparison of solutions from present theory and experimental results on critical load of an SMC-R50 composite with a midplane delamination (L = 3 in., h = 0.22 in.).

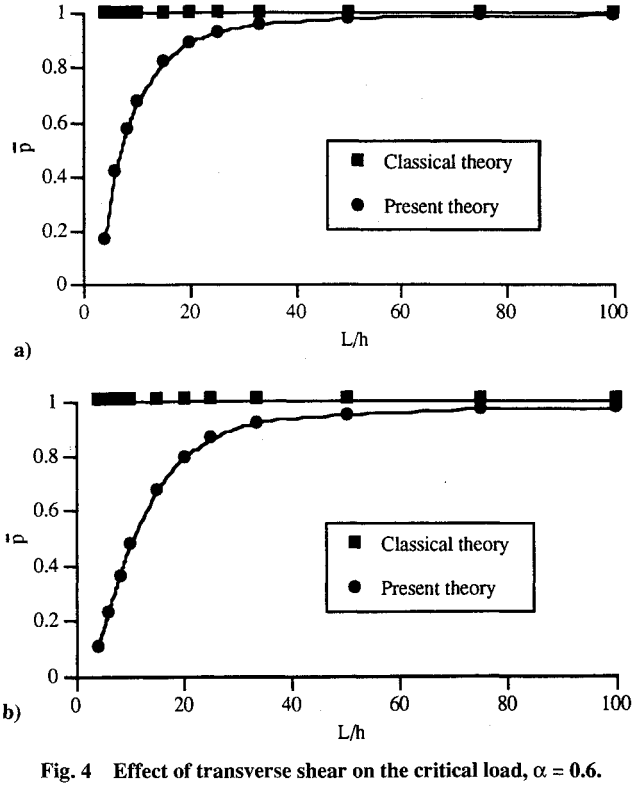

Fig. 4 Effect of transverse shear on the critical load, α = 0.6.

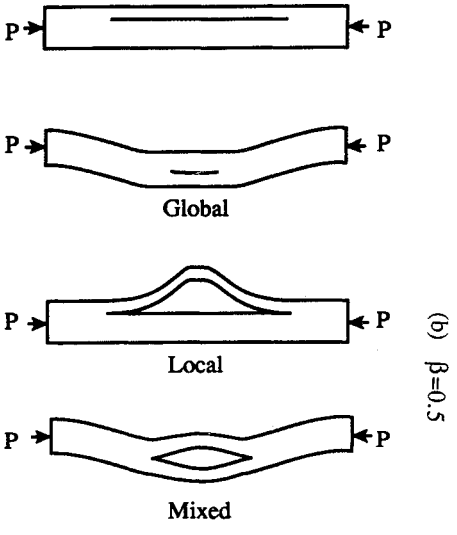

Fig. 5 Buckling modes for a delaminated composite.

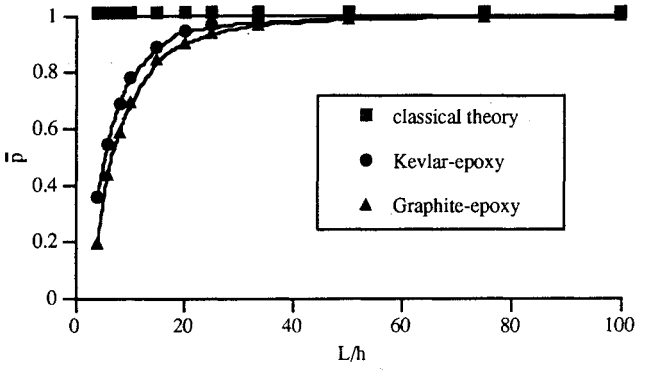

Fig. 6 Comparison of transverse shear effect with variations in material properties, β = 0.25 and α = 0.8.

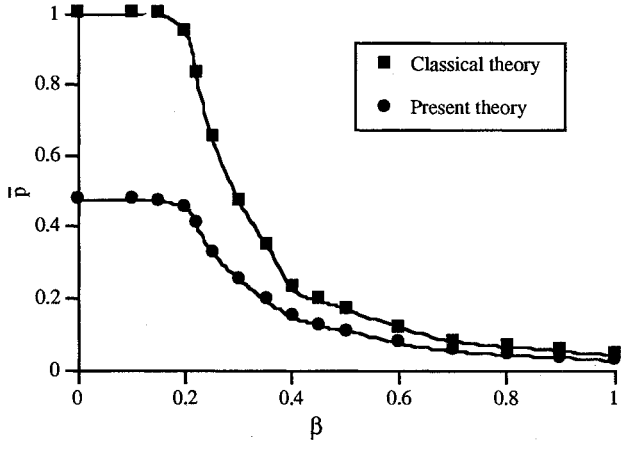

Fig. 7 Effect of transverse shear on critical load, L/h = 10 and α = 0.6.

where E, G, and ν represent, respectively, the Young's modulus, the shear modulus, and the Poisson's ratio of the material. The superscripts L and T denote longitudinal and transverse direction, respectively. The numerical results of variation of critical load with delamination length, obtained using the present theory, are compared with those obtained from experiments as shown in Fig. 3. The circled data points indicate the experimental data given in Ref. 10. The analytical results show excellent agreement with the experimental data over the entire range of delamination. Because the composite plate used in this example is thick (L/h = 13.6), it is expected that the present theory will enable the evaluation of trans-

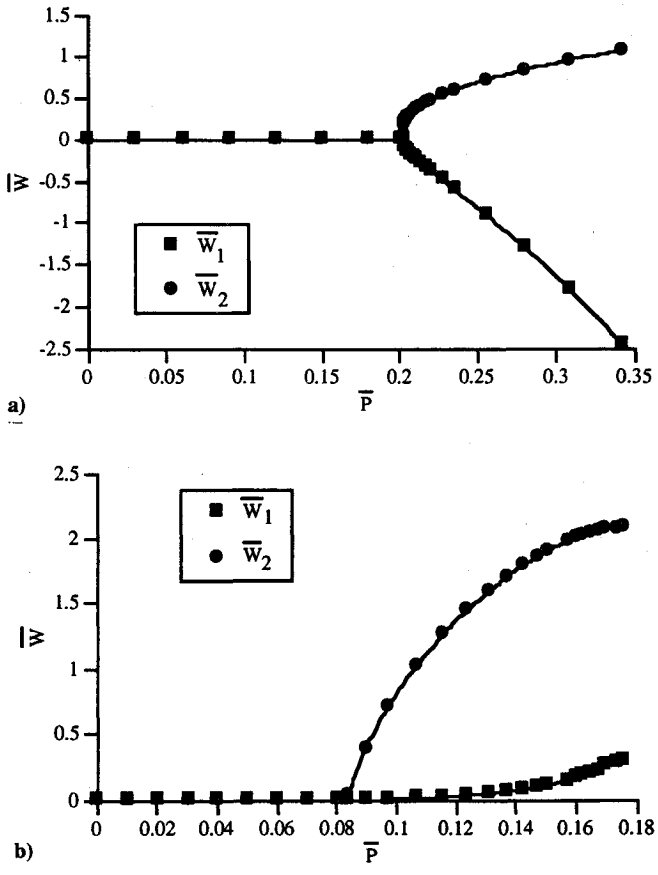

Fig. 8 Midpoint deflections of upper and lower sublaminates, L/h = 10 and α = 0.6.

verse shear effects accurately and therefore predict delamination buckling behavior realistically.

Next, analysis is performed for a clamped symmetric cross-ply plate, with pre-existing one-dimensional, through-the-width delamination. The plate is subjected to an uniform inplane compressive load along the x direction (Fig. 1). The material used is graphite/epoxy. The engineering constants, typical of this material, are as follows,

$$E_L/E_T = 40, \quad G_{LT}/E_T = 0.5, \quad \nu_{LT} = 0.25, \quad G_{TT}/G_{LT} = 1$$

Results for the critical loads are obtained for laminates with a [0 deg/90 deg/0 deg]$_{10}$ stacking sequence. The critical load distribution, $\bar{p}$, is plotted over a range of the length-to-thickness ratio, L/h, in Fig. 4a for β = 0.5 and in Fig. 4b for β = 0.2. These results are also compared with those values obtained in Ref. 4. It is shown that the critical load computed form the classical laminate theory deviates substantially from those derived using the proposed theory, particularly for cases involving lower length-to-thickness (L/h) ratios. Even at a L/h ratio of 20, at which the classical laminate theory is generally regarded to be accurate for isotropic materials, a deviation of 18% is observed in the value of the critical load. The extent of deviation is also affected by the buckling mode of the delaminated plate. It is clear from Fig. 4 that the transverse shear effect is larger in the case of β = 0.2. This can be explained as follows. In the β = 0.2 case, buckling begins with a mixed mode (combined local and global, see Fig. 5), whereas in the β = 0.5 case, local buckling is dominant. This observation is similar to that reported by Kardomateas and Schmueser in Ref. 6.

Some parametric studies are performed to investigate the effect of material properties. Figure 6 shows a comparison of the present theory with the classical laminate theory for two different materials, graphite-epoxy and Kevlar-epoxy. The engineering constants for Kevlar-epoxy are as follows.

$$E_L/E_T = 15.6, \quad G_{LT}/E_T = 0.56, \quad \nu_{LT} = 0.35, \quad G_{TT}/G_{LT} = 1$$

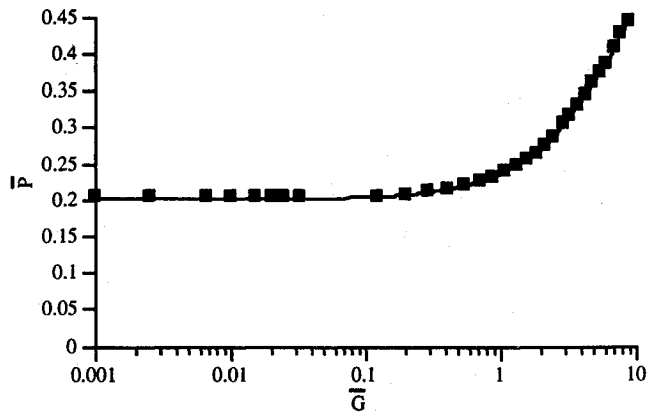

Fig. 9 Variation of energy release rate with compressive axial load, L/h = 10 and α = 0.6.

As seen from Fig. 6, the larger deviation of results, from the classical laminate theory, occurs for graphite-epoxy with a higher tensile-to-transverse modulus ratio (E_L/E_T) and a higher transverse-to-shear modulus ratio (E_T/G_{LT}), which is expected. Because these two ratios are generally large for most composite materials, it appears that the transverse shear effect becomes a very significant factor in assessing the delamination buckling behavior of laminates.

A comparison of the shear effect on the normalized critical load, $\bar{p}$, with changes in the magnitude of the delamination length parameter, β, is presented in Fig. 7. The delamination is positioned symmetrically, in the axial direction. It is seen that the transverse shear effect becomes smaller as the delamination length increases. This can be explained as follows. For short delamination lengths, global buckling is dominant, whereas for relatively longer lengths, local buckling of the delaminated layer occurs first. This phenomenon is also true for the results that include the transverse shear effect.

Figure 8 illustrates the normalized midpoint deflections of both upper and lower sublaminates, $\bar{W}_1$ and $\bar{W}_2$, for a wide range of normalized axial compressive loads $\bar{P}$. Note that $\bar{W}_1 = (W_0 + W_1)/h$, $\bar{W}_2 = (W_0 + W_2)/h$ and $\bar{P} = 3(1-\nu_{LT}\nu_{TL})pL^2/\pi^2 E_L h^3$. The delamination parameters used are L/h = 10 and α = 0.6, where $\alpha = 2h_1/h$ (Fig. 1). It is observed that the axial compressive load can be significantly greater than the critical buckling load. It must also be noted that for the case of β = 0.2 (Fig. 8a), mixed buckling occurs. Therefore, the midpoint deflections of both the upper layer and the lower substrate obviously grow in opposite directions as the compressive load increases. However, for the case of β = 0.5 (Fig. 8b), local buckling is dominant. Therefore, in this case, the midpoint deflection of the upper layer increases rapidly, although the midpoint deflection of the bottom substrate is negligible over a relatively wide range. The reason for these two deflections remaining in same direction in the latter case is that the boundary conditions considered are clamped at both ends.

The transverse shear effect is included in computing the energy release rate. The variations of the normalized axial compressive load $\bar{P}$ with the nondimensionalized energy release rate, given by $\bar{G} = 12(1-\nu_{LT}\nu_{TL})GL_4/E_L h^5$, are shown in Fig. 9. The delamination parameters used are L/h = 10 and α = 0.6. It is clear that at the initial postbuckling range, the energy release rate increases rapidly, but after the axial load reaches a certain value, the rate of increase reduces. Once the energy release rate exceeds the magnitude of the fracture toughness of the material, the delamination growth begins. From Fig. 9, it is observed that delamination growth is more likely to occur in the case of β = 0.2 than in the case of β = 0.5 because in the former case a mixed buckling mode is dominant.

Conclusions

A new higher order plate theory is developed to study the delamination buckling, postbuckling, and growth problem in composite laminates. The refined displacement field proposed in this

theory is capable of both representing displacement discontinuity conditions at the interface of the existing delamination as well as satisfying the transverse shear stress-free conditions at surfaces and at the delamination interface. The buckling load and the post-buckling solutions are governed by a set of nonlinear equations. Numerical investigations of the transverse shear effect on critical buckling load are performed. A numerical example is given to allow comparisons with experimental data. A paramatric study is also presented on the postbuckling behavior and on delamination growth. The following important observations are made from this study:

1) The present theory provides an alternative, adequate framework for analysis of composite laminates with delaminations. Particularly, the theory is expected to obtain the accurate displacement distributions with lower computational cost for engineering practice.

2) For laminated composite plates, the transverse shear effect on delamination buckling is significant.

3) The results of proposed theory show excellent agreement with available experimental data for the composite plate.

4) The delamination buckling mode plays important role in delamination buckling, postbuckling, and growth problems.

It must be noted that the theory can also be used to investigate multiple delaminations by modifying the present displacement field.

Appendix A: Identified Higher Order Terms

For $N = 4$, the identified higher order terms are given as follows.

$$U_{03} = -\frac{4}{3h^2}(U_{01} + W_{0,x})$$

$$V_{03} = -\frac{4}{3h^2}(V_{01} + W_{0,y})$$

$$U_{04} = -\frac{2}{h^2}U_{02}$$

$$V_{04} = -\frac{2}{h^2}V_{02}$$

$$U_{13} = -\frac{4}{3h^2\alpha^2}[(1-\alpha)(U_{01} + W_{0,x}) + h\alpha(1-\alpha)(U_{02} + U_{12}) + (1-\alpha+\alpha^2)(U_{21} + W_{1,x})]$$

$$V_{13} = -\frac{4}{3h^2\alpha^2}[(1-\alpha)(V_{01} + W_{0,y}) + h\alpha(1-\alpha)(V_{02} + V_{12}) + (1-\alpha+\alpha^2)(V_{21} + W_{1,y})] \tag{A1}$$

$$U_{14} = -\frac{2(1-\alpha)}{h^3\alpha^2}\left[U_{01} + W_{0,x} + h\alpha\left(\frac{U_{12}}{1-\alpha} + U_{02}\right) + U_{11} + W_{1,x}\right]$$

$$V_{14} = -\frac{2(1-\alpha)}{h^3\alpha^2}\left[V_{01} + W_{0,y} + h\alpha\left(\frac{V_{12}}{1-\alpha} + V_{02}\right) + V_{11} + W_{1,y}\right]$$

$$U_{23} = -\frac{4}{3h^2\alpha^2}[(1+\alpha)(U_{01} + W_{0,x}) + h\alpha(1+\alpha)(U_{02} + U_{12}) + (1+\alpha+\alpha^2)(U_{21} + W_{1,x})]$$

$$V_{23} = -\frac{4}{3h^2\alpha^2}[(1+\alpha)(V_{01} + W_{0,y}) + h\alpha(1+\alpha)(V_{02} + V_{12}) + (1+\alpha+\alpha^2)(V_{21} + W_{1,y})]$$

$$U_{24} = \frac{2(1+\alpha)}{h^3\alpha^2}\left[U_{01} + W_{0,x} + h\alpha\left(\frac{U_{22}}{1+\alpha} + U_{02}\right) + U_{21} + W_{2,x}\right]$$

$$V_{24} = \frac{2(1+\alpha)}{h^3\alpha^2}\left[V_{01} + W_{0,y} + h\alpha\left(\frac{V_{22}}{1+\alpha} + V_{02}\right) + V_{21} + W_{2,y}\right]$$

with

$$\alpha = 2h_1/h \tag{A2}$$

Appendix B: Governing Equations

The governing equations of the problem are as follows:

$$\delta U_{00}: \; N^{(0)}_{11,x} + N^{(0)}_{61,y} = 0$$

$$\delta V_{00}: \; N^{(0)}_{61,x} + N^{(0)}_{21,y} = 0$$

$$\delta W_0: \; N^{(0)}_{51,x} + N^{(0)}_{41,y} + N^{(0)}_{11}W_{0,xx} + 2N^{(0)}_{61}W_{0,xy} + N^{(0)}_{21}W_{0,yy} + \frac{4}{3h^2}[N^{(0)}_{14,xx} + 2N^{(0)}_{64,xy} + N^{(0)}_{24,yy} - 3(N^{(0)}_{53,x} + N^{(0)}_{43,y})] = 0$$

$$\delta U_{01}: \; N^{(0)}_{12,x} + N^{(0)}_{62,y} - N^{(0)}_{51} - \frac{4}{3h^2}(N^{(0)}_{14,x} + N^{(0)}_{64,y} - 3N^{(0)}_{53}) = 0 \tag{B1}$$

$$\delta V_{01}: \; N^{(0)}_{62,x} + N^{(0)}_{22,y} - N^{(0)}_{41} - \frac{4}{3h^2}(N^{(0)}_{64,x} + N^{(0)}_{24,y} - 3N^{(0)}_{53}) = 0$$

$$\delta U_{02}: \; N^{(0)}_{13,x} + N^{(0)}_{63,y} - 2N^{(0)}_{52} - \frac{2}{h^2}(N^{(0)}_{15,x} + N^{(0)}_{65,y} - 4N^{(0)}_{54}) = 0$$

$$\delta V_{02}: \; N^{(0)}_{63,x} + N^{(0)}_{23,y} - 2N^{(0)}_{42} - \frac{2}{h^2}(N^{(0)}_{65,x} + N^{(0)}_{25,y} - 4N^{(0)}_{44}) = 0$$

$$(x, y) \in \Omega - \Omega_d$$

$$\delta U_{00} \text{ or } \delta U_{i0}: \; N^{(i)}_{11,x} + N^{(i)}_{61,y} = 0$$

$$\delta V_{00} \text{ or } \delta V_{i0}: \; N^{(i)}_{61,x} + N^{(i)}_{21,y} = 0$$

$$\delta W_0 \text{ or } \delta W_i: \; N^{(i)}_{51,x} + N^{(i)}_{41,y} + N^{(i)}_{11}(W_0 + W_1)_{,xx} + 2N^{(i)}_{61}(W_0 + W_1)_{,xy} + N^{(i)}_{21}(W_0 + W_1)_{,yy} + \frac{4}{3h^2}g_{i1}(\alpha) \times [N^{(i)}_{14,xx} + 2N^{(i)}_{64,xy} + N^{(i)}_{24,yy} - 3(N^{(i)}_{53,x} + N^{(i)}_{43,y})] + \frac{2}{h^3}g_{i2}(\alpha)[N^{(i)}_{15,xx} + 2N^{(i)}_{65,xy} + N^{(i)}_{25,yy} - 4(N^{(i)}_{54,x} + N^{(i)}_{44,y})] = 0$$

$$\delta U_{01} \text{ or } \delta U_{i1}: \; N^{(i)}_{12,x} + N^{(i)}_{62,y} - N^{(i)}_{51} - \frac{4}{3h^2}g_{i1}(\alpha)(N^{(i)}_{14,x} + N^{(i)}_{64,y} - 3N^{(i)}_{53}) - \frac{2}{h^3}g_{i2}(\alpha)(N^{(i)}_{15,x} + N^{(i)}_{65,y} - 4N^{(i)}_{54}) = 0$$

$$\delta V_{01} \text{ or } \delta V_{i1}: \; N^{(i)}_{62,x} + N^{(i)}_{22,y} - N^{(i)}_{41} - \frac{4}{3h^2}g_{i1}(\alpha)(N^{(i)}_{64,x} + N^{(i)}_{24,y} - 3N^{(i)}_{43}) - \frac{2}{h^3}g_{i2}(\alpha)(N^{(i)}_{65,x} + N^{(i)}_{25,y} - 4N^{(i)}_{44}) = 0$$

$$\delta U_{02} \text{ or } \delta U_{i2}: \quad N^{(i)}_{13,x} + N^{(i)}_{63,y} - 2N^{(i)}_{52} - \frac{2}{h^2} g_{i4}(\alpha)(N^{(i)}_{15,x} + N^{(i)}_{65,y} - 4N^{(i)}_{54}) - \frac{4}{3h} g_{i3}(\alpha)(N^{(i)}_{14,x} + N^{(i)}_{64,y} - 3N^{(i)}_{53}) = 0$$

$$\delta V_{02} \text{ or } \delta V_{i2}: \quad N^{(i)}_{63,x} + N^{(i)}_{23,y} - 2N^{(i)}_{42} - \frac{2}{h^2} g_{i4}(\alpha)(N^{(i)}_{65,x} + N^{(i)}_{25,y} - 4N^{(i)}_{44}) - \frac{4}{3h} g_{i3}(\alpha)(N^{(i)}_{64,x} + N^{(i)}_{24,y} - 3N^{(i)}_{43}) = 0$$

$$i = 1, 2; \qquad (x, y) \in \Omega_d \tag{B2}$$

where the stress resultants $N^{(k)}_{ij}$ are defined by

$$N^{(k)}_{ij} = \int_{z_1}^{z_2} \sigma_i z^{j-1}\, dz, \quad \begin{cases} z_1 = -h/2, \ z_2 = h/2; & \text{if } k = 0 \\ z_1 = -h/2, \ z_2 = h_1; & \text{if } k = 1 \\ z_1 = h_1, \ z_2 = h/2; & \text{if } k = 2 \end{cases} \tag{B3}$$

and the function $g_{ij}(\alpha)$, $i = 1, 2$; $j = 1, \ldots, 4$, are as follows:

$$g_{11} = \frac{1 - \alpha + \alpha^2}{\alpha^2}, \quad g_{12} = \frac{1 - \alpha}{\alpha^2}, \quad g_{13} = \frac{1 - \alpha}{\alpha}$$

$$g_{14} = g_{24} = \frac{1}{\alpha}, \quad g_{21} = \frac{1 + \alpha + \alpha^2}{\alpha^2}, \quad g_{22} = \frac{1 + \alpha}{\alpha^2} \tag{B4}$$

$$g_{23} = \frac{1 + \alpha}{\alpha}$$

The boundary conditions are

Geometric	Force
U_{00}	$N^{(0)}_{11} n_x + N^{(0)}_{61} n_y$
V_{00}	$N^{(0)}_{61} n_x + N^{(0)}_{21} n_y$
W_0	$[N^{(0)}_{51} + \frac{4}{3h^2}(N^{(0)}_{14,x} + N^{(0)}_{64,y} - 3N^{(0)}_{53} + N^{(0)}_{11} W_{,x} + N^{(0)}_{61} W_{,y})] n_x + [N^{(0)}_{41} + \frac{4}{3h^2}(N^{(0)}_{64,x} + N^{(0)}_{24,y} - 3N^{(0)}_{53} + N^{(0)}_{61} W_{,x} + N^{(0)}_{21} W_{,y})] n_y$
$W_{0,x}$	$N^{(0)}_{14} n_x + N^{(0)}_{64} n_y$
$W_{0,y}$	$N^{(0)}_{64} n_x + N^{(0)}_{24} n_y$
U_{01}	$(N^{(0)}_{12} - \frac{4}{3h^2} N^{(0)}_{14}) n_x + (N^{(0)}_{62} - \frac{4}{3h^2} N^{(0)}_{64}) n_y$
V_{01}	$(N^{(0)}_{62} - \frac{4}{3h^2} N^{(0)}_{64}) n_x + (N^{(0)}_{22} - \frac{4}{3h^2} N^{(0)}_{24}) n_y$
U_{02}	$(N^{(0)}_{13} - \frac{2}{h^2} N^{(0)}_{15}) n_x + (N^{(0)}_{63} - \frac{2}{h^2} N^{(0)}_{65}) n_y$
V_{02}	$(N^{(0)}_{63} - \frac{2}{h^2} N^{(0)}_{65}) n_x + (N^{(0)}_{23} - \frac{2}{h^2} N^{(0)}_{25}) n_y$

$$(x, y) \in \Gamma_\Omega \tag{B5}$$

The corresponding continuity conditions are

Force:

$$N^{(0)}_{11} - N^{(1)}_{11} - N^{(2)}_{11} = 0$$

$$N^{(0)}_{61} - N^{(1)}_{61} - N^{(2)}_{61} = 0$$

$$N^{(0)}_{21} - N^{(1)}_{21} - N^{(2)}_{21} = 0$$

$$N^{(0)}_{12} - N^{(1)}_{12} - N^{(2)}_{12} = 0$$

$$N^{(0)}_{62} - N^{(1)}_{62} - N^{(2)}_{62} = 0$$

$$N^{(0)}_{22} - N^{(1)}_{22} - N^{(2)}_{22} = 0$$

$$N^{(0)}_{13} - N^{(1)}_{13} - N^{(2)}_{13} - \frac{2}{h^2}[N^{(0)}_{15} - g_{14}(\alpha) N^{(1)}_{15} - g_{24}(\alpha) N^{(2)}_{15}] + \frac{4}{3h}[g_{13}(\alpha) N^{(1)}_{14} - g_{23}(\alpha) N^{(2)}_{14}] = 0$$

$$N^{(0)}_{63} - N^{(1)}_{63} - N^{(2)}_{63} - \frac{2}{h^2}[N^{(0)}_{65} - g_{14}(\alpha) N^{(1)}_{65} - g_{24}(\alpha) N^{(2)}_{65}] + \frac{4}{3h}[g_{13}(\alpha) N^{(1)}_{64} - g_{23}(\alpha) N^{(2)}_{64}] = 0$$

$$N^{(0)}_{23} - N^{(1)}_{23} - N^{(2)}_{23} - \frac{2}{h^2}[N^{(0)}_{25} - g_{14}(\alpha) N^{(1)}_{25} - g_{24}(\alpha) N^{(2)}_{25}] + \frac{4}{3h}[g_{13}(\alpha) N^{(1)}_{24} - g_{23}(\alpha) N^{(2)}_{24}] = 0$$

$$N^{(0)}_{14} - g_{11}(\alpha) N^{(1)}_{14} - g_{24}(\alpha) N^{(2)}_{14} + \frac{4}{3h}[g_{12}(\alpha) N^{(1)}_{15} - g_{22}(\alpha) N^{(2)}_{15}] = 0$$

$$N^{(0)}_{64} - g_{11}(\alpha) N^{(1)}_{64} - g_{24}(\alpha) N^{(2)}_{64} + \frac{4}{3h}[g_{12}(\alpha) N^{(1)}_{65} - g_{22}(\alpha) N^{(2)}_{65}] = 0$$

$$N^{(0)}_{24} - g_{11}(\alpha) N^{(1)}_{24} - g_{24}(\alpha) N^{(2)}_{24} + \frac{4}{3h}[g_{12}(\alpha) N^{(1)}_{25} - g_{22}(\alpha) N^{(2)}_{25}] = 0$$

$$N^{(0)}_{51} - N^{(1)}_{51} - N^{(2)}_{51} - \frac{4}{h^2}[N^{(0)}_{53} - g_{11}(\alpha) N^{(1)}_{53} - g_{21}(\alpha) N^{(2)}_{53}] + \frac{8}{h^3}[g_{12}(\alpha) N^{(1)}_{54} - g_{22}(\alpha) N^{(2)}_{54}] - \frac{4}{3h^2}(N^{(1)}_{11} W_{1,x} + N^{(1)}_{61} W_{1,y} + N^{(2)}_{11} W_{2,x} + N^{(2)}_{61} W_{2,y}) = 0$$

$$N^{(0)}_{41} - N^{(1)}_{41} - N^{(2)}_{41} - \frac{4}{h^2}[N^{(0)}_{43} - g_{11}(\alpha) N^{(1)}_{43} - g_{21}(\alpha) N^{(2)}_{43}] + \frac{8}{h^3}[g_{12}(\alpha) N^{(1)}_{44} - g_{22}(\alpha) N^{(2)}_{44}] - \frac{4}{3h^2}(N^{(1)}_{61} W_{1,x} + N^{(1)}_{21} W_{1,y} + N^{(2)}_{61} W_{2,x} + N^{(2)}_{21} W_{2,y}) = 0$$

Geometric:

$$U_{ij} = 0, \quad V_{ij} = 0, \quad W_i = 0$$

$$W_{i,x} = 0, \quad W_{i,y} = 0 \qquad i = 1, 2; \quad j = 0, 1, 2$$

$$(x, y) \in \Gamma_{\Omega_d} \tag{B6}$$

Acknowledgment

This research was supported by the U.S. Army Research Office under Grant DAAH04-93-G-0043.

References

[1]Chai, H., Babcock, C. D., and Krauss, W. G., "One Dimensional Modeling of Failure in Delaminated Laminates," *International Journal of Solids and Structures*, Vol. 17, No. 11, 1981, pp. 1069–1083.

[2]Chai, H., and Babcock, C. D., "Two-dimensional Modeling of Failure in Laminated Plates by Delamination Buckling," *Journal of Composite Materials*, Vol. 19, Jan. 1985, pp. 67–98.

[3]Whicomb, J. D., "Finite Element Analysis of Instability Related Delamination Growth," *Journal of Composite Materials*, Vol. 15, Sept. 1981, pp. 403–426.

[4]Sallam, S., and Simitses, G. J., "Delamination Buckling and Growth of Flat, Cross-ply Laminates," *Journal of Composite Structures*, Vol. 4, No. 4, 1985, pp. 361–381.

[5]Lo, K. H., Christensen, R. M., and Wu, E. M., "A High-order Theory of Plate Deformation, Part 2: Laminated Plates," *Journal of Applied Mechanics*, Vol. 44, Dec. 1977, pp. 669–676.

[6]Kardomateas, G. A., and Schmueser, D. W., "Buckling and Postbuckling of Delaminated Composites Under Compressive Loads Including Transverse Shear Effects," *AIAA Journal*, Vol. 26, No. 3, 1988, pp. 337–343.

[7]Chen, H. P., "Shear Deformation Theory for Compressive Delamination Buckling and Growth," *AIAA Journal*, Vol. 29, No. 5, 1991, pp. 813–819.

[8]Barbero, E. J., and Reddy, J. N., "Modeling of Delamination in Composite Laminates Using a Layer-wise Plate Theory," *International Journal of Solids and Structures*, Vol. 28, No. 3, 1991, pp. 373–388.

[9]Vinson, J. R., and Sierakowski, R. L., *The Behavior of Structures Composed of Composite Materials*, Martinus Nijhoff, Dordrecht, The Netherlands, 1987, pp. 45–49.

[10]Wang, S. S., Zahlan, N. M., and Suemasu, H., "Compressive Stability of Delaminated Random Short-Fiber Composites, Part II–Experimental and Analytical Results," *Journal of Composite Materials*, Vol. 19, July 1985, pp. 317–333.